

INTERNATIONAL SOCIETY FOR SOIL MECHANICS AND GEOTECHNICAL ENGINEERING



This paper was downloaded from the Online Library of the International Society for Soil Mechanics and Geotechnical Engineering (ISSMGE). The library is available here:

<https://www.issmge.org/publications/online-library>

This is an open-access database that archives thousands of papers published under the Auspices of the ISSMGE and maintained by the Innovation and Development Committee of ISSMGE.

Influence of the end friction on the response of triaxial and plane strain clay samples

Influence du frottement limite sur le comportement des échantillons d'argile tri-axiales et d'état de déformation plane

Dunja Perić & Shu Su

Department of Civil Engineering, Kansas State University, Manhattan, Kansas, 66506-5000, USA

ABSTRACT

Focus of this study is on the heterogeneities in laboratory clay samples, which are caused by the presence of completely rough end platens. Non-uniformities in the stress and strain fields of Weald clay samples subjected to drained triaxial and plane strain compressions are assessed by finite element simulations. A three-invariant Cam clay model with volumetric hardening/softening is used to describe the stress-strain behavior of normally consolidated and heavily overconsolidated clay samples. Even though the whole sample nominal stress-strain response is not substantially altered by the friction at the sample-platen interface significant heterogeneities evolve inside the samples. They are caused primarily by non-uniform distributions of the mean effective stress. Local vertical strains at the central portion of the samples greatly exceed 25%, the strain of homogeneously deforming specimens with smooth ends. At the same time the top and bottom outside edges experience small strains and significant stiffening effects due to concentration of the mean effective stress and corresponding decrease in the void ratio. Thus, critical state is reached only at the central part of the samples with the rough ends. In addition, while different types of loading are experienced by different locations inside overconsolidated samples such as a plastic softening, plastic hardening and elastic loading/unloading, in the case of normally consolidated samples all points appear to undergo plastic hardening. The location near the top centerline always experiences some elastic unloading, which is more pronounced in triaxial compression. It is expected that these heterogeneities may play a significant role in initiating the strain localization.

RÉSUMÉ

Le point central de cette étude est sur les hétérogénéités dans les échantillons d'argile de laboratoire, qui sont provoqués par la présence des platines d'extrémité complètement rugueuses. Les non-uniformités dans les champs de contraintes et de déformations dans des échantillons d'argile de Weald soumis à des compressions tri-axiales et autres de déformation plane drainés sont évaluées par des simulations d'éléments finis. Un modèle à trois-invariants d'argile de Cam avec durcissement/assouplissement volumétrique est utilisé pour décrire le comportement de contrainte-déformation des échantillons d'argile normalement consolidé et fortement surconsolidé. Malgré que la réponse nominale de contrainte-déformation n'est pas sensiblement changée par le frottement des platines, des hétérogénéités importantes se produisent à l'intérieur des échantillons. Ils sont provoqués principalement par des distributions non-uniformes des contraintes effectives moyennes à l'intérieur des échantillons. Les déformations verticales locales à la partie centrale des échantillons excèdent 25% la déformation des spécimens à déformation homogène utilisant des platines d'extrémités lisses. En même temps, le bord extérieur supérieur est soumis à des déformations petites et un effet de durcissement important dû à une concentration des contraintes effectives moyennes et une diminution du rapport de porosité. Ainsi, l'état critique est atteint seulement dans la partie centrale des échantillons avec extrémités rugueuses. En outre, alors que différents types de chargement sont sentis à des endroits différents dans les échantillons surconsolidés, tels que assouplissement plastique, durcissement plastique et chargement/déchargement élastique, dans le cas des échantillons normalement consolidés tous les points semblent subir un durcissement plastique. L'endroit près de la ligne centrale supérieure subit un déchargement élastique, qui est davantage prononcé dans les tests à compression triaxiales. Les hétérogénéités jouent un rôle significatif dans le lancement de la localisation de tension.

1 INTRODUCTION

Laboratory procedures for soil testing along with the corresponding techniques for interpretation of results have been a hindrance to further improvements in the soil property characterization and numerical modeling. Difficulties in the interpretation of experimental results arise primarily due to the following two reasons: (1) unknown inhomogeneities and disturbances within the soil samples as naturally formed earth materials, and (2) the influence of end conditions such as the sample-platen friction, and load inclination and eccentricity. These conditions are likely to produce non-uniformities in the stress and strain states within the specimens thus making them more susceptible to early development of shear bands, which cause a sudden and severe strength loss that would not otherwise be observed. However, in the past constitutive properties have been usually determined based on the assumption that laboratory specimens deform uniformly.

The primary focus of this study is to numerically investigate non-uniformities in the laboratory specimens of Weald clay that are loaded in drained conventional triaxial and plane strain compression in the presence of the full sample-platen friction. A constitutive model employed herein is a three-invariant modified Cam clay model, which is suitable for nearly isotropically consolidated clays that exhibit a normal to light overconsolidation. The model employs a volumetric hardening/softening and it is based on the associated flow rule.

2 NUMERICAL ANALYSIS

Numerical modeling was conducted with the commercial finite element code ABAQUS. The three-invariant Cam-clay model (Perić and Ayari, 2002) is one of the standard constitutive models that are implemented in ABAQUS. This model enables a fully coupled flow-deformation analysis. An identical finite element mesh was used to model both, plane strain and

axisymmetric experiments. Eight-node quadrilateral plane strain and axisymmetric elements with the full integration were used. Thus, it is tacitly assumed that the specimen preserves its circular or rectangular cross-sections throughout the loading. This assumption is reasonable for initially perfectly homogeneous specimens subjected to symmetric loading and boundary conditions. A quarter-sample mesh is shown in Fig.1 along with the corner Gauss points A, C and D at which various quantities are subsequently displayed. All samples have the overall aspect ratio (height to width or diameter) of 2:1. Horizontal displacements were prevented at all nodes located on the left boundary due to the symmetry, as well as along the top boundary due to a completely rough top platen.

The model parameters were previously determined by Carter (1982) based on the assumption that the experimental results reported by Wood (1990) were obtained from homogeneously deforming specimens. These parameters were subsequently adjusted herein by matching a numerically obtained nominal stress-strain response of samples subjected to a full sample-platen friction with the experimental results. The final values of the model parameters were Poisson ratio (ν) of 0.3, the plastic (λ) and elastic (κ) compressibilities of 0.081 and 0.033 respectively, the slope of the critical state line in compression (M) of 0.86, the intercept of the isotropic consolidation line (N) of 2.101 and the ellipticity (\bar{e}) of 0.78. Neither the shear nor the bulk modulus was specified since they are both mean stress dependent. In addition, the coefficient of permeability (k) of 1.097×10^{-7} m/day was used. All samples were loaded numerically in the mixed control mode starting from the homogeneous stress state corresponding to either the isotropic or plane strain consolidation to the selected stress levels. In all cases vertical strain rate was constant whereby the nominal vertical strain of 25% was reached in 2000 days. This strain rate ensured that the largest excess pore pressure within the sample did not exceed 0.5 kPa.

Four different cases were studied including two samples loaded in the plane strain compression (PS) and another two samples loaded in the conventional triaxial compression (CTC). For each type of loading two stress histories were considered: two normally consolidated samples with the past maximum mean effective stress in the isotropic compression equal to 207 kPa, and two heavily overconsolidated samples with the past maximum mean effective stress in the isotropic compression equal to 828 kPa and overconsolidation ratios ranging from 3.3 to 3.9.

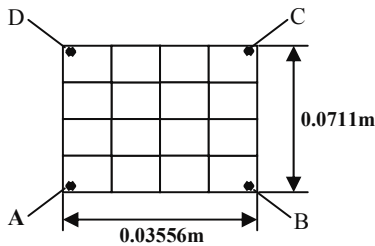


Figure 1. A schematic of the quarter-sample mesh for a sample with 2:1 aspect ratio

3 RESULTS

Results for normally consolidated samples are presented in Figures 2 to 5. Clearly, all samples are deforming nonuniformly whereby the central portion (point A) exhibits vertical strain levels that are greatly in excess of the nominal vertical strain of 25%. In the case of normally consolidated samples all three points (A, C and D) undergo plastic hardening. However, it can be seen from Figures 3, 4 and 5 that only point A reaches the critical state. It is noted that a modified stress ratio $\bar{\eta}$ is defined as follows:

$$\bar{\eta} = \eta g(\theta), \quad \text{where } \eta = q/p', \quad (1)$$

and $g(\theta)$ is a so-called Willam-Warnke function (Willam and Warnke, 1974) that originates from the third invariant of the deviator stress tensor, while θ is Lode's angle. Thus, the path traversed by the point A is similar to the path of the homogeneously deforming sample (with smooth end platens) as well as to the experimental data that were recorded globally on the sample level. The mean effective stress at point C, which is located at the lower and upper outside edges, undergoes a significant increase, thus causing a corresponding decrease in the void ratio (Fig. 4). This behavior is more pronounced in the plane strain loading. Finally, point D is subjected to much smaller load than points A and C. In the conventional triaxial test the soil at point D elastically unloads towards the end of the test.

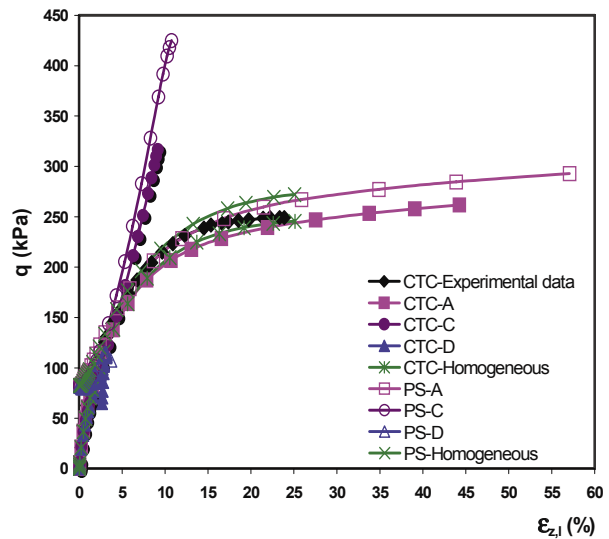


Figure 2. Deviator stress versus local vertical strain for normally consolidated samples

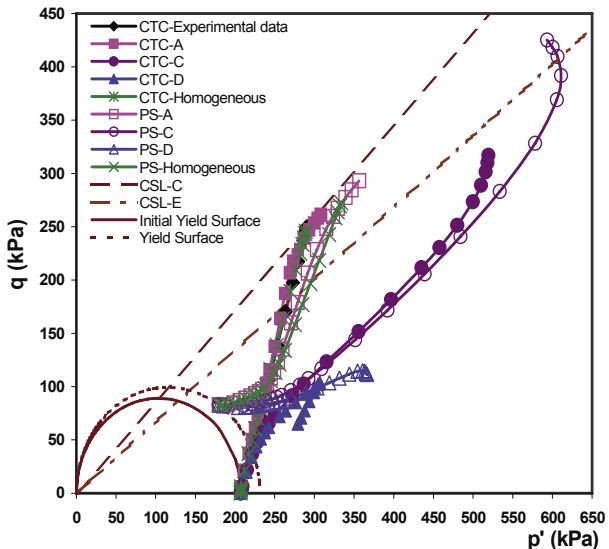


Figure 3. Deviator stress versus mean effective stress for normally consolidated samples

Results for overconsolidated samples are presented in Figures 6 to 9. Even though initially all three points (A, C and D) undergo an elastic loading they subsequently exhibit

different types of responses. While plastic yielding at point A is followed by a softening to the critical state, at point C it is followed by a plastic hardening in the heavily overconsolidated plane strain sample. Thus, the upper and lower outer edges experience hardening effect due to increase in the mean effective stress similarly to normal consolidated samples discussed previously. However, in the case of overconsolidated samples the stiffening effect in point C is insignificant in the triaxial sample (Fig. 6). Point A traverses a path that is different from the path of a homogeneously deforming sample (Fig. 6, 8 and 9). Point D remains in the elastic regime during the entire course of loading and it undergoes elastic unloading towards the end, which is more pronounced in triaxial test.

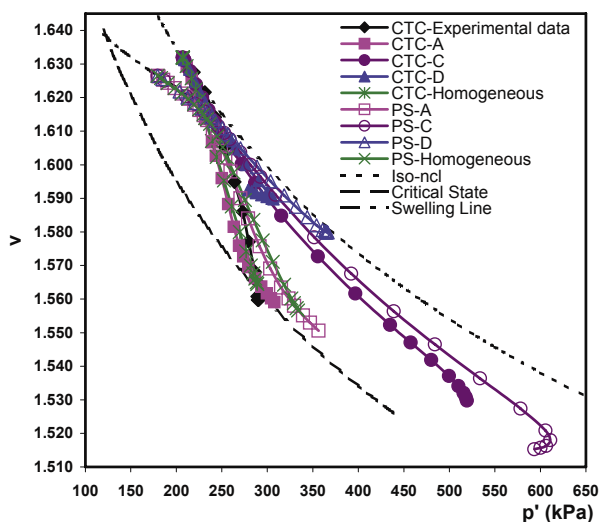


Figure 4. Specific volume versus mean effective stress for normally consolidated samples

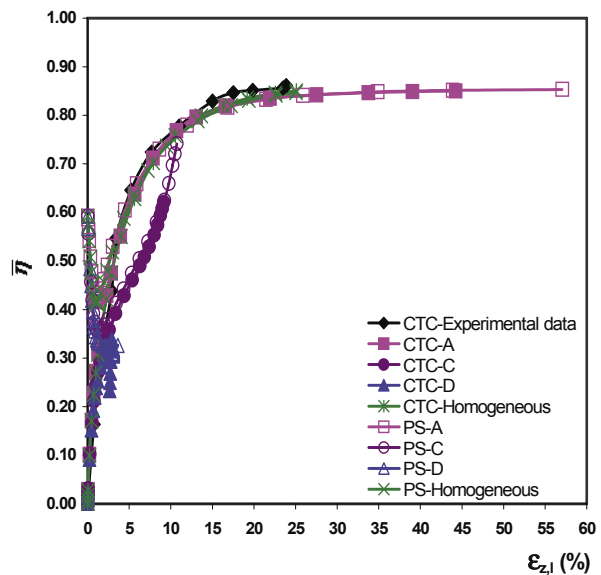


Figure 5. Modified stress ratio versus local vertical strain for normally consolidated samples

Vertical strain fields at the time of 2000 days are shown in Figure 10 for overconsolidated samples from where it is evident that strain distribution within the samples is highly non-uniform. Local vertical strains of 25 % that correspond to the nominal vertical strain are reached only within two narrow strips in both cases, plane strain and triaxial compressions. While the central part of the sample is experiencing large strain,

the upper part is undergoing very small strains. At midheight location magnitude of vertical strains decreases in the outward direction more so in the plane strain case.

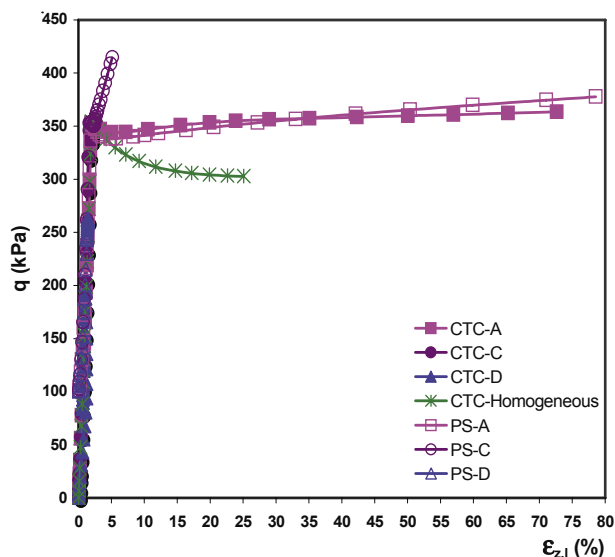


Figure 6. Deviator stress versus local vertical strain for overconsolidated samples

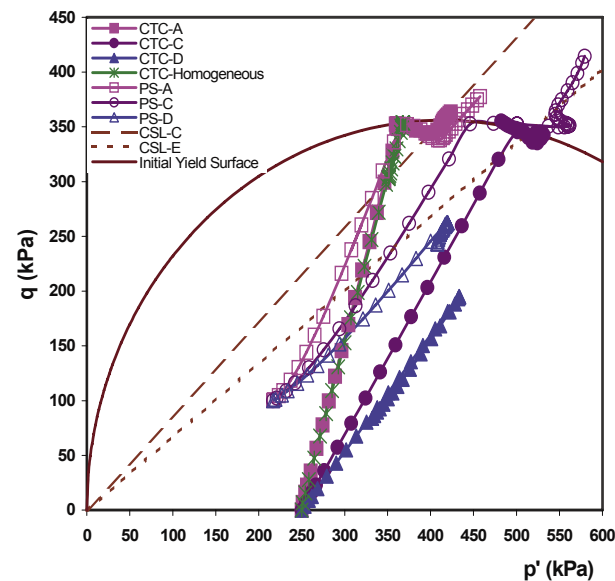


Figure 7. Deviator stress versus mean effective stress for overconsolidated samples

4 CONCLUSIONS

A nominal stress-strain response of a whole sample remains nearly unaffected by the presence of rough end platens. This can be concluded based on the very small difference between the Cam clay model parameters that were obtained for samples with smooth ends (Carter, 1982) and with rough ends herein. However, the presence of the full friction at the sample-platen interface introduces a significant heterogeneity in the stress and strain fields of triaxial and plane strain samples. In all cases stress concentration occurs in terms of all components of the stress tensor at the upper outside edge (point C). Thus, the soil is compressed the most at this location resulting in the smallest void ratio. Truly large strains are experienced in the central part

of the sample and it may be necessary to use a fully fledged large strain theory to obtain more proper response. While the critical state is generally reached within the centrally located portion of the sample the soil near the top surface is far away from the critical state even at the nominal vertical strain of 25%.

It is expected that the heterogeneous stress and strain rates that is included by the presence of rough end platens could have implications for the strain localization. However, the onset of localization is highly dependent on the constitutive description. In the present case a strain softening is the necessary condition for the onset of the shear localization due to an associated plasticity.

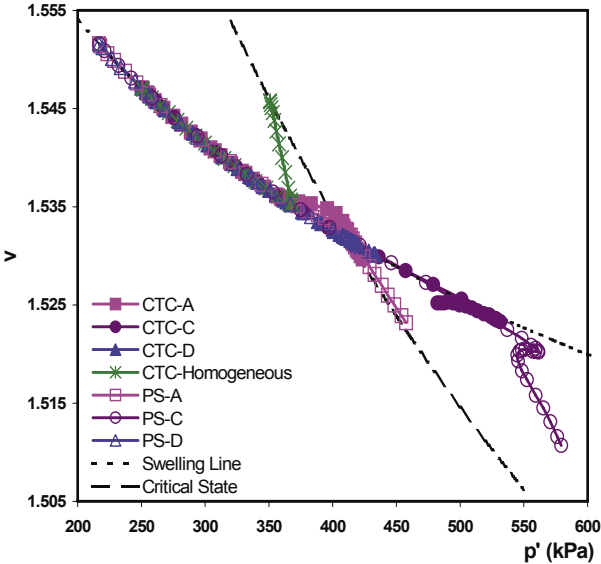


Figure 8. Specific volume versus mean effective stress for overconsolidated samples

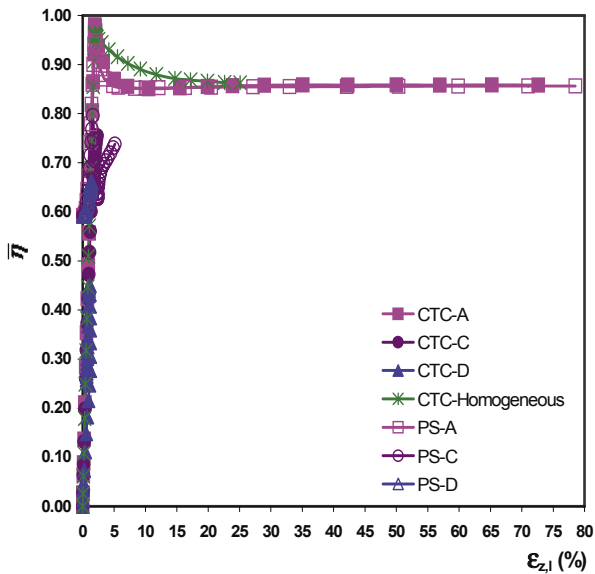
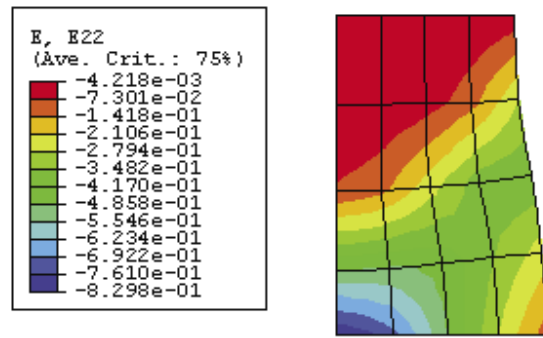
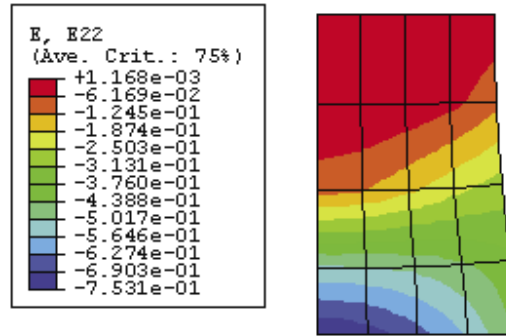


Figure 9. Modified stress ratio versus local vertical strain for overconsolidated samples



A)



B)

Figure 10. Vertical strain fields in overconsolidated A) plane strain, and B) conventional triaxial samples. Strains in this figure are shown on the quarter sample mesh and they are negative in compression due to the sign convention employed in ABAQUS.

In addition, it is likely that degree of a departure from the axisymmetric stress state also has influence on the onset of shear banding. More detailed localization analysis is underway. It must be noted that the standard finite element solutions presented herein are not valid beyond the possible onset of strain localization due to a spurious mesh dependence.

ACKNOWLEDGEMENTS

Hibbitt, Karlsson, provided the ABAQUS software under an academic license & Sorensen, Inc. Financial support for this research was provided by Kansas State University.

REFERENCES

- Albert, R. A. A. and Rudnicki, J. W. 2000. Non-uniformity of stress and deformation in axisymmetric finite element models of Tennessee marble. Pp. 999-1006 in Pacific Rocks 2000: Proceedings of the Fourth North American Rock Mechanics Symposium, Girard, Liebman and Doe (Eds).
- Carter, J. P. 1982. Prediction of the non-homogeneous behaviour of clay in the triaxial test. *Geotechnique*, 32, 55-58.
- Perić, D. and Ayari, M. A. 2002. On the analytical solutions for the three-invariant Cam clay model. *Int. J. Plasticity*, 18, 1061-1082.
- Willam, K. J. And Warnke, E. P. 1974. Constitutive model for triaxial behavior of concrete. In: Colloquium on Concrete Structures Subjected to Triaxial Stresses, ISMES, Bergamo.
- Wood, D.M. 1990. *Soil Behaviour and Critical State Soil Mechanics*. Cambridge University Press, Cambridge, 462p.